Supplementary Material

Optical quantal analysis of synaptic transmission in wild-type and *rab3*-mutant *Drosophila melanogaster* motor axons

Einat S. Peled and Ehud Y. Isacoff

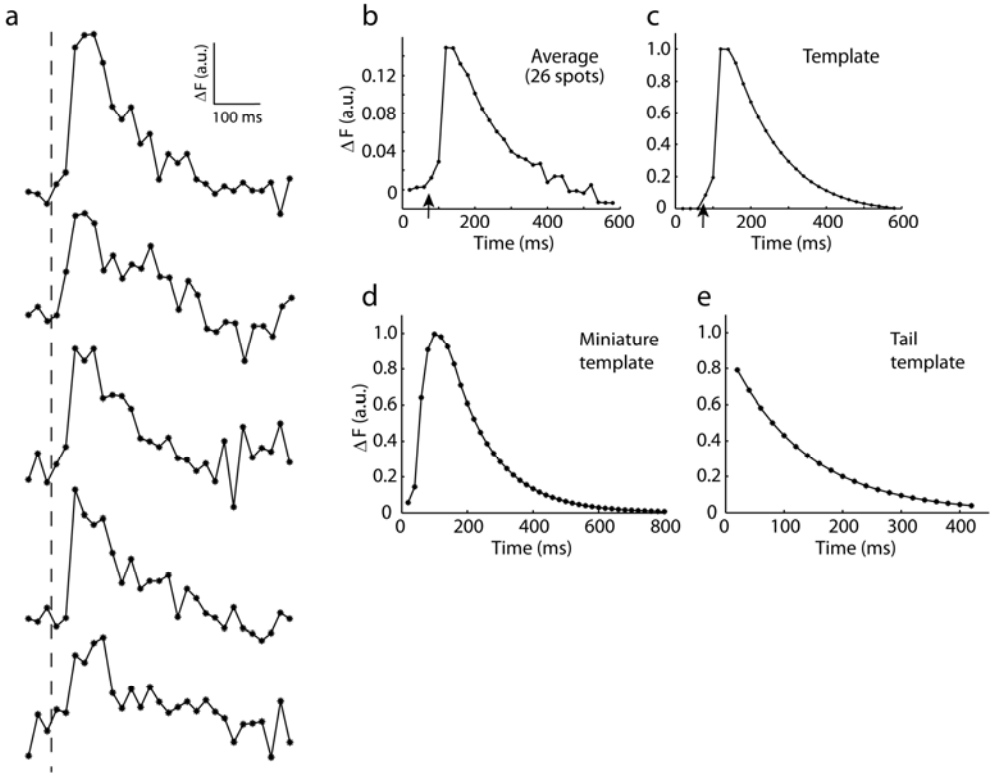

Supplementary Figure 1 ΔF template response traces used for activity detection. (**a**) Examples of ΔF traces at five different transmission sites in response to single nerve stimulus. Dashed line marks the time of nerve stimulation. (**b**) Average of 40 ΔF traces as in (**a**), obtained from 26 different transmission sites across 10 stimulation trials. (**c**) ΔF template trace for activity detection. This template was obtained by fitting the fluorescence decay in (**b**) to a double exponential. (**b**, **c**) Black arrows mark time of nerve stimulation. (**d**) ΔF template trace for detecting spontaneous activity, obtained by averaging and fitting 36 spontaneous ΔF traces, as in parts (**a**–**c**). (**e**) The fluorescence decay part of the template trace in (**d**) was used as a template for detecting miniature 'tails' (see **Methods**).

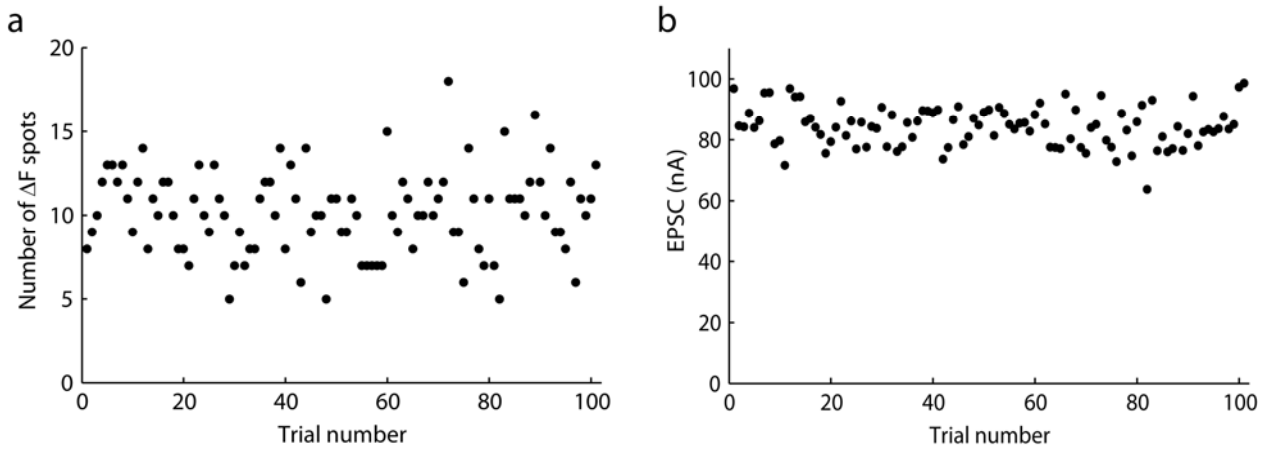

Supplementary Figure 2 The number of postsynaptic ΔF spots evoked by a single action potential in the NMJ fluctuates about a stable value. (**a**) Number of ΔF spots evoked in the NMJ shown in **Fig. 1a** is plotted against trial number. (**b**) EPSCs from the same experiment plotted against trial number.

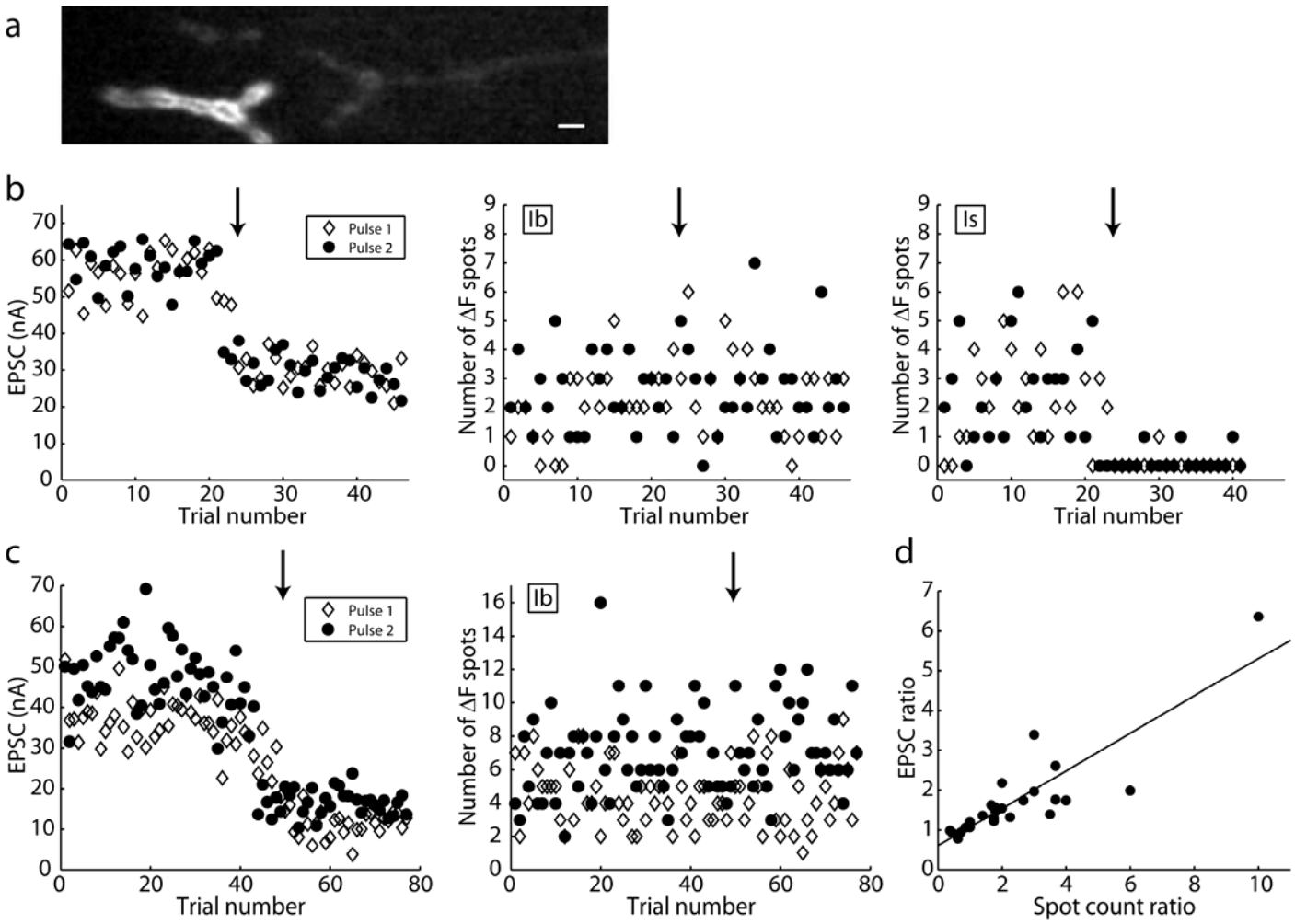

Supplementary Figure 3 Separating the contributions of type Is and Ib boutons to the EPSC paired-pulse facilitation ratio. (**a**) Single-plane confocal image of a muscle 4 NMJ, showing both type Ib boutons (large and bright at lower left) and type Is boutons (faint fluorescence extending from right to central descending branch and upper branch toward left). (**b**) Left: EPSCs evoked by the first and second stimulation pulses in the NMJ from (**a**). A drop in the EPSCs after pair 20 leaves ΔFs in Ib uninterrupted (middle panel), whereas ΔFs in the Is boutons disappear (right panel). Note, response counts are low since a large portion of both the Is and Ib branches was out of the field of view. (**c**) An example of a second NMJ where Ib responses continue uninterrupted (right) after a drop in the EPSCs (left). Is boutons were not

included in the field of view, to allow imaging of a larger portion of the Ib boutons. Since no change was detected in the Ib responses, we assume that the drop in ESPCs is due to a failure of the Is axonal branch, as in part (**b**). (**d**) Correlation between EPSC ratio (pulse 2 / pulse 1) and Ib ΔF spot-count ratio for trials that occurred after Is failure from part (**c**) ($r = 0.87$, $p < 0.0001$ correlation analysis). (**b**, **c**) Black arrows mark the times of Is failure. Scale bar, 5 μm (**a**).

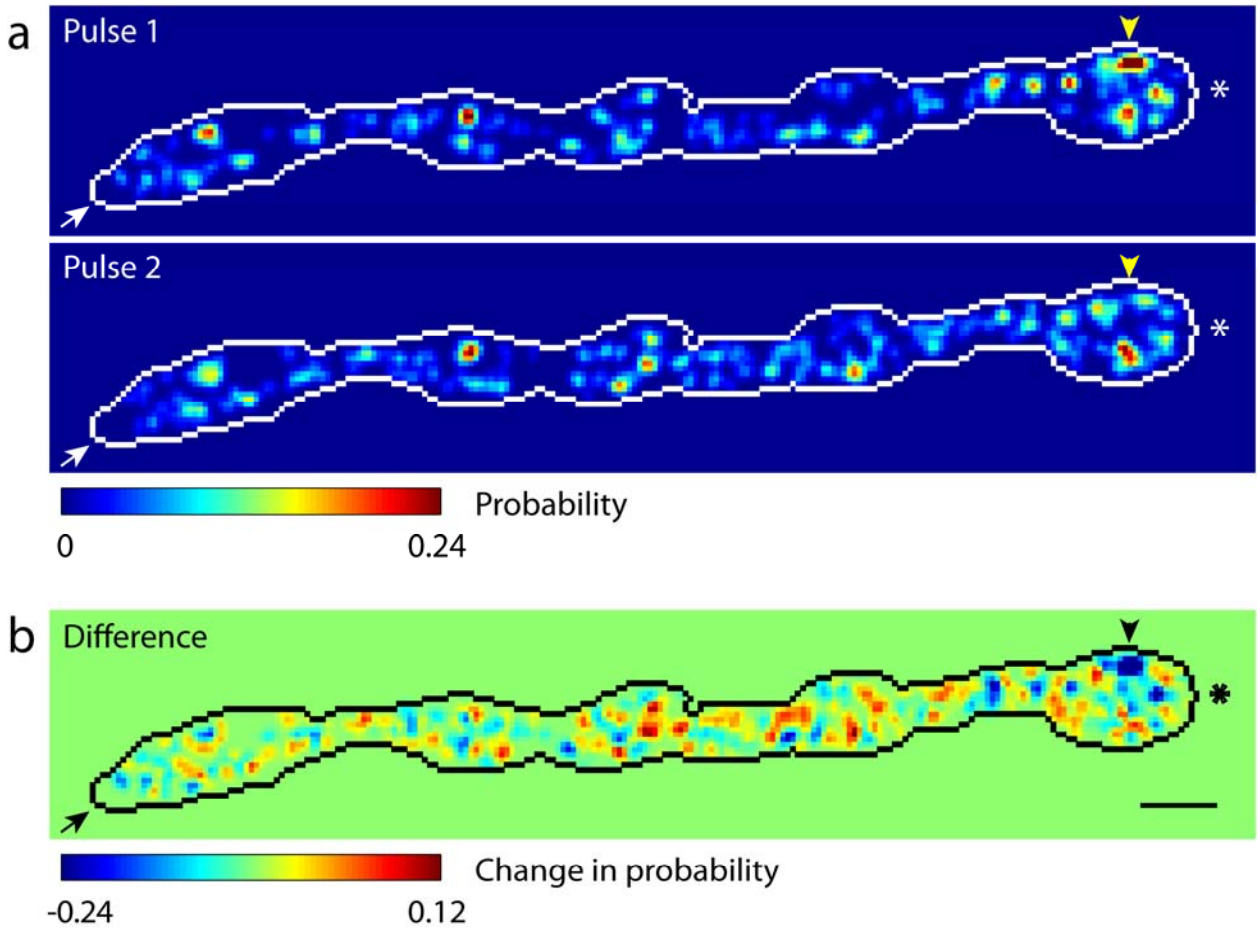

Supplementary Figure 4 A second example of paired-pulse imaging showing change in aggregate release probabilities from pulse 1 to pulse 2. (**a**) Maps of release probabilities to pulses 1 and 2. Yellow arrowhead marks a release site that shows a large decrease in probability (see **Fig. 7b** for an example of a release site that shows a large increase in probability). (**b**) Map of the changes in release probabilities (difference between probability maps for pulse 2 and pulse 1, from (**a**)). Black arrowhead marks the depressing release site. (**a**, **b**) Proximal and distal boutons are labeled by arrow and asterisk, respectively. Scale bar, 5 μm (**a**, **b**).

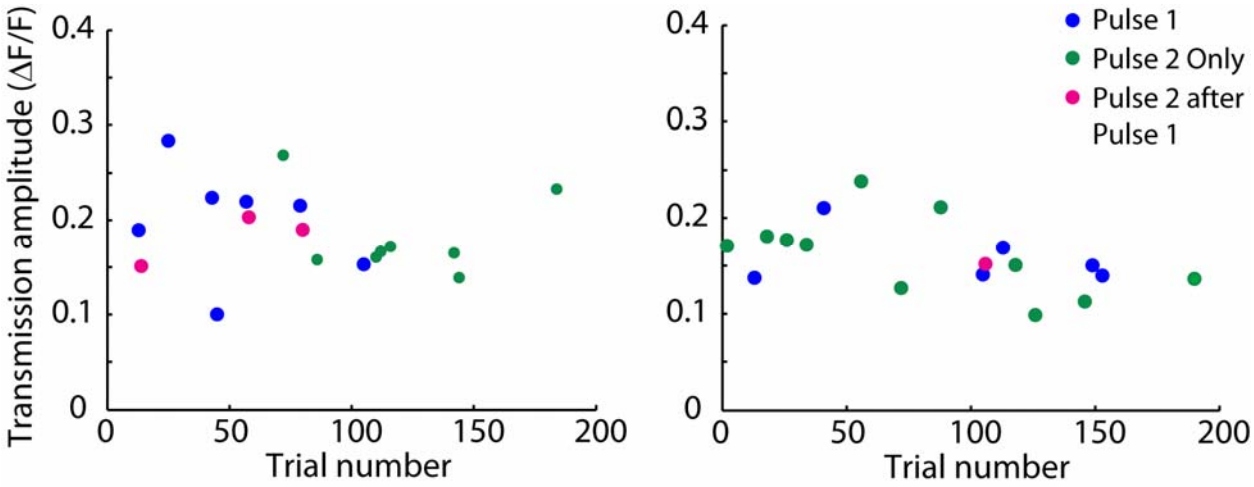

Supplementary Figure 5 Similar ΔF/F values for first and second pulse responses within the same release site. Left and right panels: examples of ΔF/F imaging amplitudes evoked at two different release sites in response to pulses 1 and 2 of paired-pulse stimulation. Responses in 21 selected release sites in 3 preparations had a mean amplitude (ΔF/F) of 0.19 ± 0.01 (mean ± s.e.m) for the pulse 1 response, a slightly smaller amplitude (0.17 ± 0.01; $p < 0.02$, paired t-test) for a pulse 2 response that follows a pulse 1 response at the same site, and an equal pulse 2 response (0.19 ± 0.01; $p = 0.48$, paired t-test) when no first-pulse response occurred.

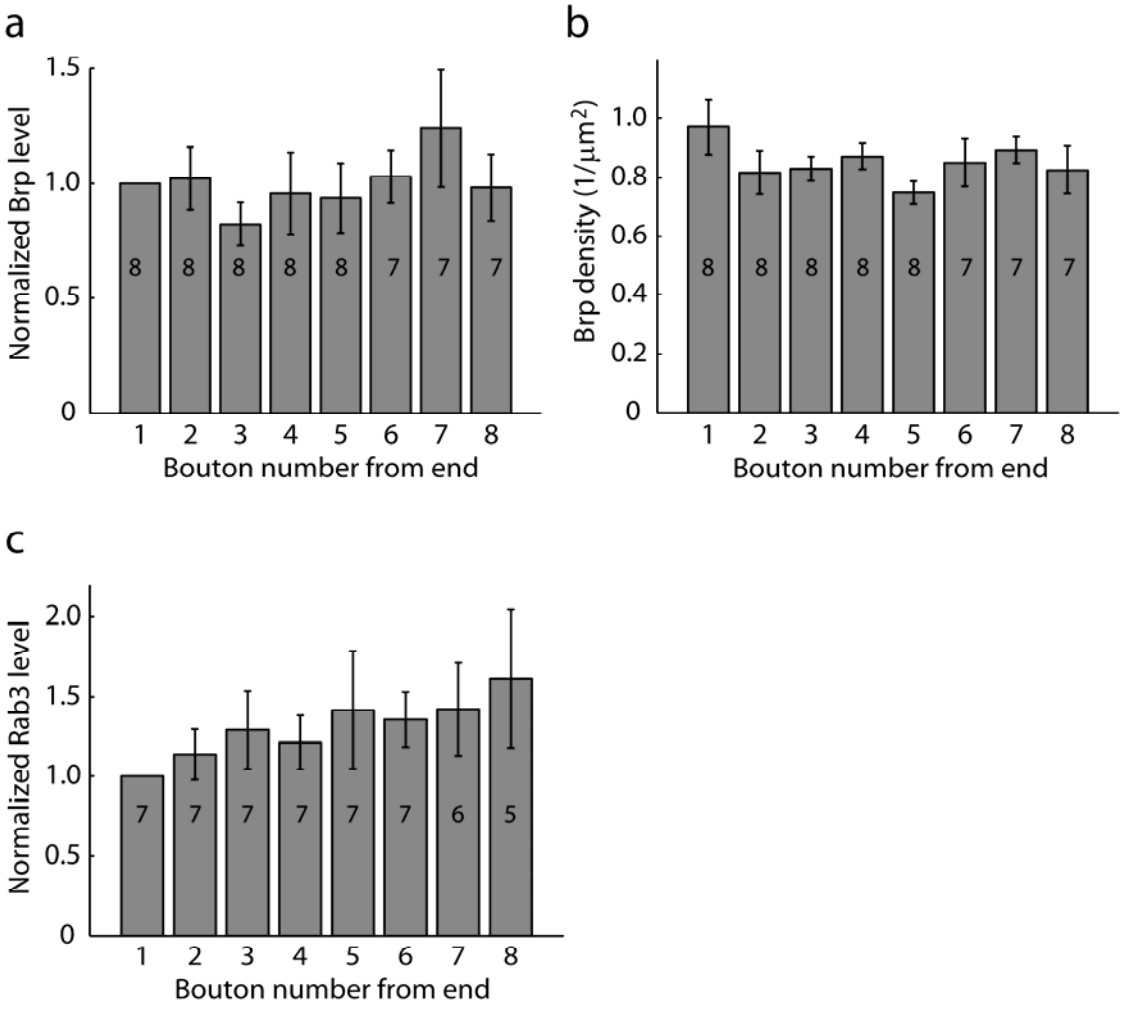

Supplementary Figure 6 Brp and Rab3 levels are uniform along the length of axonal branches. Wild-type NMJs were stained for the presynaptic protein Brp or for Rab3. Rab3 and Brp intensity, as well as Brp density values, were determined for all boutons along the length of axonal branches. (**a**) Average Brp intensity in a bouton is plotted against bouton location from end of branch. Counts are normalized to the distal bouton. (**b**) Average Brp density in a bouton is plotted against bouton location from end of branch. (**a, b**) n = 8 branches, 5 NMJs. (**c**) Average Rab3 intensity in a bouton is plotted against bouton location from end of branch. Counts are normalized to distal bouton (n = 7 branches, 6 NMJs). (**a**–**c**) Values are mean ± s.e.m, numbers in bars are number of boutons averaged.

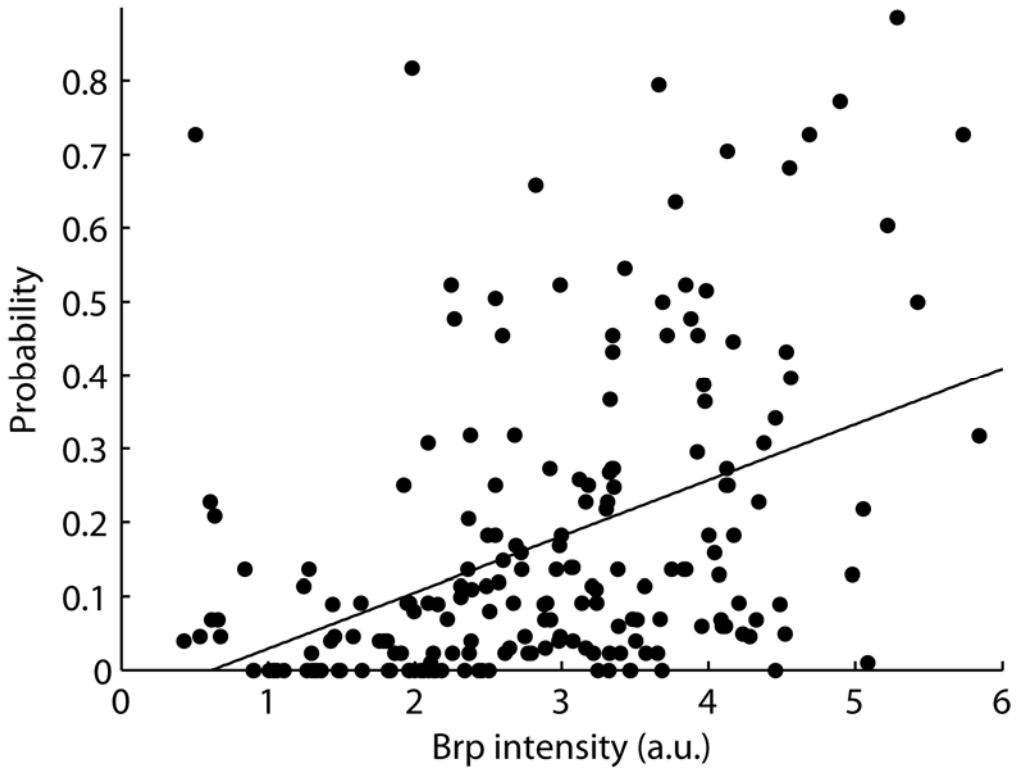

Supplementary Figure 7 In *rab3*-mutant NMJs, release probability increases with increasing levels of Brp (raw data of **Fig. 8c**). Release probability is plotted against the Brp level at individual release sites (n = 198 release sites from 2 NMJs, $r = 0.43$, $p < 0.0001$ correlation analysis).

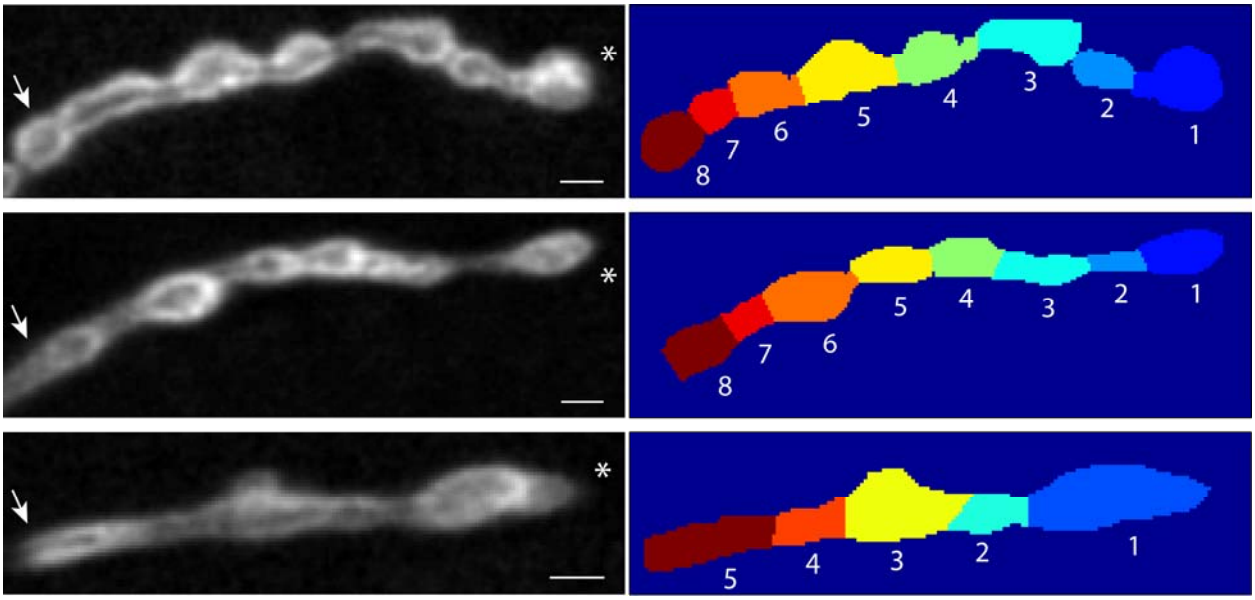

Supplementary Figure 8 Three examples of the segmentation of axonal branches into bouton-areas, for the comparison of release probabilities and levels of activity at different locations along the axon branch. Left panels are grayscale images of basal SynapGCamp2 fluorescence in three NMJs (corresponding to the release probability maps in **Fig. 5a**). Proximal and distal boutons are labeled by arrow and asterisk, respectively. Right panels show the segmentation of the axonal branches to individual bouton-areas. Each area on the right roughly corresponds to one bouton, and was selected manually based on the morphology of the axonal branches. Very small boutons, or boutons that appeared to be budding from much larger boutons, were clumped together with their larger neighbors, to minimize variation in the size of bouton-areas. Small boutons that appeared to be budding from distal boutons were either ignored or clumped together with the distal boutons. Scale bar, 5 μm.

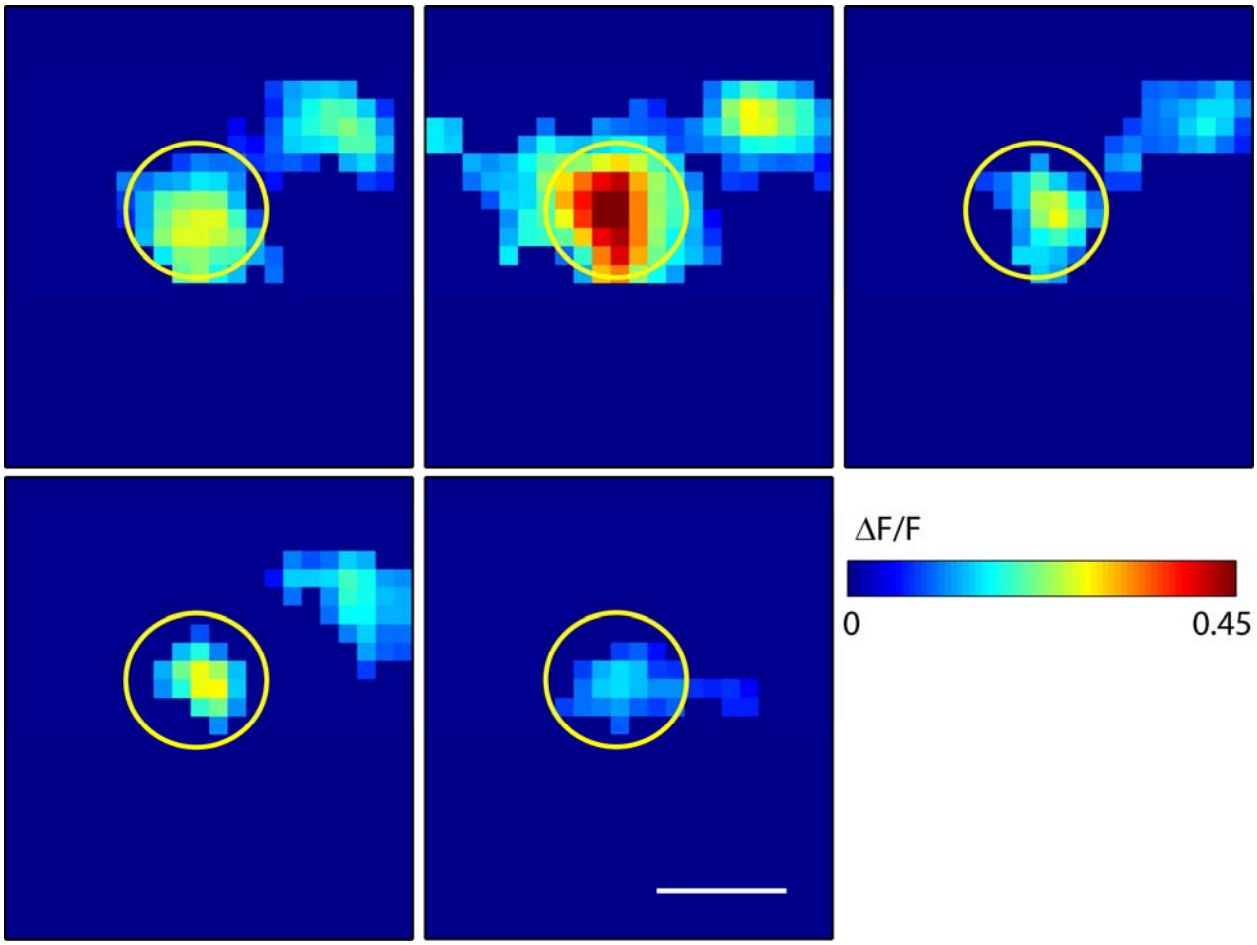

Supplementary Figure 9 Five ΔFs at same release site evoked by single stimuli. These examples represent isolated spots (having minimal overlap with responses from neighboring sites) which would be selected for determining transmission amplitudes (**Fig. 3d**,**e**, **Fig. 8e**,**f**, and **Supplementary Fig. 5**). Yellow circle marks location of release site. Scale bar, 2.5 μm.

NMJ #	QC	% Ib contribution	% Ib captured in imaging	Expected ΔF spot count	Average ΔF spot count	% detected ΔF spots
1	88.2	23	37	7.5	6.8	91
2	36.9	37	43	5.9	2.2	37
3	57.3	57	58	18.9	21	111
4	34.6	30	44	4.6	4.5	98
5	64.8	9	42	2.4	2.6	108

Supplementary Table 1 An estimation of the percentage of synaptic activity that is reported by SynapGCaMP2 imaging. Usually over 90% of activity in the type Ib branch selected for imaging will be detected. The table compares the average ΔF spot count and the expected count for five different preparations. The expected ΔF spot count is the average number of release events that we expected to occur within the imaging field of view (only part of one type Ib terminal was typically within the field of view and only type Ib transmission was analyzed, not type Is). We estimated the expected ΔF spot count by calculating the quantal content (QC) for each recording and then multiplying it by the fraction of release events that would occur within the imaged type Ib branch. This fraction was estimated as: (expected relative contribution of type Ib terminals to the QC) × (fraction of Ib terminals that were within the field of view). QC was determined by dividing EPSP by mEPSP amplitudes, with correction for possible non-linear summation[1]. The relative contribution of type-Ib terminals to QC was determined as the ratio of average EPSC amplitudes without and with type Is contribution (EPSC(Ib) / EPSC(Ib + Is)), measured after and before drop-out of the type Is axon from transmission (see examples in **Supplementary Fig. 3b** and **c**). Fraction of Ib terminals that were within the field of view was calculated as: area of the imaged Ib branch / total area of type Ib terminals present in the NMJ.

SUPPLEMENTARY MOVIE LEGENDS

Supplementary Movie 1 Single action-potential evoked responses in the NMJ of **Fig. 1**. Images are single-plane grayscale confocal scans of the SynapGCaMP2 Ca^{2+} sensor fluorescence in the NMJ. The field of view contains both type Ib (center) and type Is (lower right corner) axonal branches. Image scan time is 40 ms/frame. The movie shows 10 pairs of images, corresponding to 10 separate nerve-stimulation trials that were taken 8 seconds apart. Each pair of images includes one image of basal fluorescence, taken 1 second before nerve stimulation, and one Ca^{2+}-response image, taken after nerve stimulation, at the peak of the fluorescence response (confocal scan starting 40 ms after nerve stimulation). Scale bar, 10μm.

Supplementary Movie 2 Spontaneous activity in the NMJ of **Fig. 2.** Single-plane color coded confocal images of fluorescence changes (ΔF/F) in the NMJ. The movie includes two series of 53 images each. In each series, images were acquired continuously at 20 ms/frame. Time between the start of the first and second series is 16 seconds. ΔF/F range in images is 0 – 0.5. Scale bar, 5 μm.

Supplementary Movie 3. Responses to paired-pulse stimulation (NMJ of **Fig. 7**). Single-plane color coded confocal images of fluorescence changes (ΔF/F) in the NMJ in response to paired-pulse stimulation with an interval of 50 ms between pulse 1 and pulse 2. The movie shows responses to one paired-pulse stimulation trial. Images were acquired continuously, at a scanning speed of 10 ms/frame. Green squares indicate the times of peak ΔF response to pulses 1 and 2. Total movie time is 250 ms. ΔF/F range in images is 0 – 0.5. Scale bar, 5 μm.

SUPPLEMENTARY TEXT

Higher release probabilities in *rab3* mutants are consistent with multiple electron dense T-bars in the mutant active zones

The higher release probabilities in *rab3*-mutant NMJs are consistent with the finding that the mutant active zones frequently contain multiple electron-dense T-bars, in contrast to wild-type active zones, which typically contain a single T-bar[2]. We found that the median release probability is 0.07 in wild-type and 0.27 in *rab3* mutants. If each T-bar could support one vesicle fusion event per presynaptic action potential then four T-bars per active zone would be expected to have a combined probability of release of $1 - (1 - 0.07)^4$ or 0.25. While this is consistent with the reported numbers of up to five T-bars per *rab3*-mutant active-zone[2] it cannot by itself account for the even higher mutant release probabilities: about 20% of the mutant transmission sites have a probability of 0.6 or higher, which by the above logic will require twelve or more T-bars. Thus, the absence of Rab3 must play a role in regulating release probability at another additional level.

Miniature recordings in high-sucrose HL3 solution

The high-sucrose recording solution used to increase mEPSP frequency (**Fig. 2** and **Fig. 6**) continuously drove release of vesicles at a rate of ~15 Hz. This NMJ-wide release rate was unevenly distributed among release sites, with the highest release frequency that was observed at a single site (in SynapGCaMP2 imaging) being 0.16 Hz. While this frequency is higher than that evoked by even the highest probability sites (where probability = ~0.5) at a stimulation frequency of 0.1 Hz, this was only an issue for a small minority of the sites. Most of the sites had sucrose-induced spontaneous release frequency of less than 0.05 Hz and so could be readily compared to evoked release. In addition, we did not observe any sign of vesicle depletion in our recordings, as mEPSP

frequency did not decrease significantly during the course of the high-sucrose experiments.

SUPPLEMENTARY REFERENCES

1. Martin, A. R. A further study of the statistical composition on the end-plate potential. *J Physiol* **130**, 114-122 (1955).

2. Graf, E. R., Daniels, R. W., Burgess, R. W., Schwarz, T. L. & DiAntonio, A. Rab3 dynamically controls protein composition at active zones. *Neuron* **64**, 663-677 (2009).